Complexation of a Linear Polyelectrolyte with a Charged Dendrimer: Polyelectrolyte Stiffness Effects

ARTICLE *in* MACROMOLECULES · JANUARY 2010

Impact Factor: 5.8 · DOI: 10.1021/ma901988m

2 AUTHORS, INCLUDING:

Wen-de Tian
Suzhou University
20 PUBLICATIONS **347** CITATIONS

Macromolecules
ARTICLE

Macromolecules **2010**, *43*, 1575–1582 **1575**
DOI: 10.1021/ma901988m

Complexation of a Linear Polyelectrolyte with a Charged Dendrimer: Polyelectrolyte Stiffness Effects

Wen-de Tian[†] **and Yu-qiang Ma***[,†,‡]

[†]*National Laboratory of Solid State Microstructures and Department of Physics, Nanjing University, Nanjing 210093, China and* [‡]*Laboratory of Soft Condensed Matter Physics and Interdisciplinary Research, Soochow University, Suzhou 215006, China*

Received September 5, 2009; Revised Manuscript Received December 30, 2009

ABSTRACT: We employ extensive coarse-grained molecular dynamics simulations to explore the influence of rigidity of linear polyelectrolyte (PE) on the dendrimer−PE complexes. We find that the size of PE chain increases and its shape changes from oblate to prolate concomitant with the interesting conformation transformations from "coil"-like to "U"-like or "V"-like and further to "rod"-like as the stiffness of PE is increased. We also find that, as a soft nanoparticle, the changes of the size and the shape of charged dendrimer depend not only on the stiffness of PE but also on Bjerrum length of system. This can be explained in terms of two competing interaction energies: the bending energy and the electrostatic attractive energy. Furthermore, we witness that the effective charge of dendrimer exists a jump at both Bjerrum lengths studied, but the overcharge only appears at the large Bjerrum length. Moreover, we propose that there may exist an optimum stiffness of bioactive guest in the complexes for delivery and release.

I. Introduction

The search for an efficient and nontoxic vector for drug delivery and gene transfection is the main issue of the delivery of bioactive agents (e.g., drugs, RNA, DNA, and antisense sequences) to their targets.[1,2] On the other hand, medical imaging has become a very important technology in medical diagnosis and treatment. To find a safe and high-resolution agent is also a significant subject, to which scientists have intensively paid attention.[3,4] Dendrimer, a treelike macromolecule,[5] has been demonstrated to possess an immense potential in these areas due to its unique intrinsic properties, such as controlled mass, uniform structure, surface functionality, good water solubility, and biocompatibility.[6] For instance, complexes of DNA and polyamidoamide (PAMAM) dendrimers were indicated to have lower toxicity and higher transfection efficiency for gene delivery.[7] Dendrimer-functionalized shell-cross-linked iron oxide nanoparticles were synthesized and used for in vivo magnetic resonance imaging of tumors.[8] Additionally, many studies[9,10] have focused on the interaction of nanoparticles with membranes in order to understand the mechanism of delivery of "drugs" into cells and to explore the parameters for improving the targeting efficiency. It has been suggested that the size, shape, and net surface charge of nanoparticles play a very important role in their penetrating through the cell membrane.[11−14] Accordingly, it is of great significance in understanding the interactions of dendrimers as ideal nanocarriers with RNA, DNA, and other molecules. In particular, exploring the size, shape, and effective charge of charged dendrimers affected by these bioactive agents under various conditions is a very interesting issue, since it represents the very first step to understand the vehicle-mediated gene and drug delivery.

Up to now, computational techniques have been proved to be very effective in elucidating the structural properties of charged dendrimer.[15−18] However, there are only few studies paying attention to the complexes between dendrimers and linear polyelectrolytes (PEs)[19−24] though it is very crucial to understand the complexation of dendrimers with bioactive guests. The pioneering work of Welch and Muthukumar[19] studied these complexes by employing the Monte Carlo simulations as a model guest−host system for gene delivery. It was suggested that a charged dendrimer can encapsulate or interpenetrate a linear polyelectrolyte (PE) or display a unique "chain-walking" behavior depending on the solution ionic strength, size, and charge density of the dendrimer. Similarly, Lyulin et al.[21] investigated the structural aspects and dynamic behaviors of the complexes formed by a cationic dendrimer and a long anionic PE chain via Brownian dynamics simulations. They found that the PE wrapped the dendrimer surface accompanied by the decrease of the size of the dendrimer when the PE and the dendrimer had the same number of charges. They also observed the overcharging phenomenon[25,26] for longer PE chains with more charges than the neutralization of dendrimers. Among others, Lyulin et al.[22] also suggested that a sufficiently long PE attached to a dendrimer displays a very slow "non-random-walk" behavior. However, it should be stressed that the above studies employed very simplified models in which the effects of counterions were taken into account implicitly and the solvent was described as a continuum dielectric medium. The electrostatic interactions were accounted for within the Debye−Hückel approximation, which may be problematic when applied to charged dendrimers because it can easily break down as the distance of charges goes below the Bjerrum length.[23]

Very recently, Maiti and Bagchi[24] studied dendrimer−ssDNA complexes through atomistic molecular dynamics simulations with explicit counterions and water molecules. They demonstrated that the ssDNA can wrap around and significantly penetrate into the dendrimer when it has enough positive charges to neutralize the charges on the ssDNA. They also pointed out that the stability of the complexes is strongly sensitive to the ssDNA sequence because of a competition between binding enthalpy and bending rigidity of ssDNA. While their landmark

*Corresponding author. E-mail: myqiang@nju.edu.cn.

Published on Web 01/12/2010

work provides a detailed molecular level understanding of the structure and dynamics of the complexes, it should be noted that its very high computational load prohibits systematic studies of various factors that would affect the structures of the complexes, such as ionic strength and pH value. Besides, another major problem[13,23] is the limitation of time scale and length scale in atomistic methods because of their accurate nature. For these reasons, the coarse-grained (CG) model at a lower resolution, which reduces computational time considerably, is a suitable approach for studying more generic features of the charged dendrimers at a larger scale. On the other hand, if treating ions[17,18] explicitly, the CG model can go beyond the Debye−Hückel approximation. On the basis of this idea, Lyulin et al.[23] performed the extensive coarse-grained molecular dynamics simulations on the complexes formed by a cation dendrimer of the fourth generation and a relatively short anionic chain with explicit counterions as well as solvent molecules. They focused on the influence of the strength of electrostatic interactions on the properties of the complexes and paid special attention to understanding the effects of counterions and PE chains with various valencies. Their results revealed that the charged dendrimers have the ability to encapsulate guest chains and to screen them protectively from the surrounding solvent.

Although the above researches via different techniques have provided important structural information for the charged dendrimers interacting with linear PEs, a systematical study that takes into account the effect of the chain rigidity is still lacking. The present paper is aimed to explore qualitatively the impact of bioactive agents such as DNA, RNA, and drugs[27] with various rigidities on the terminally charged dendrimers in the framework of CG model, the level of which has been demonstrated to reach a state where all relevant dendrimer properties can be modeled in a realistic fashion as long as one is interested in qualitative features.[23] The remainder of the paper is organized as follows. In section II, the model and the simulation algorithm are described. In section III, the results of our simulations and discussion are presented. Finally, the conclusion is given in section IV.

II. Model and Simulation Methods

We have performed the extensive molecular dynamics simulations[18] to study the complexes of a terminally charged dendrimer and a linear PE within the framework of the freely jointed bead−spring model.[15] As for the trifunctional dendrimer, the total number N of monomers with generation G is defined by the equation $N = 3(2^{G+1} - 1) + 1$. The $G = 4$ is considered in our system. Each monomer of the terminal generation is set to carry a positive unit charge, corresponding to the protonated primary amine of a PAMAM dendrimer under near physiological pH conditions. A chain with the negatively charged monomers is chosen to represent a linear PE. Each charged monomer dissociates a monovalent counterion into the solution. Solvent molecules[18] described as Lennard-Jones (LJ) spheres are also added into the system. All the simulation systems are preserved overall charge neutrality. A schematical sketch of our model is depicted in Figure 1.

The harmonic spring potential is used to maintain the connectivity of the nearest-neighbor monomers

$$U_{\text{bond}}(r) = \frac{1}{2}K_b(\ell - \ell_0)^2 \tag{1}$$

Here, ℓ_0 denotes the bond length, which will also be used as the length unit in this text. The spring constant K_b is equal to $10^3 k_B T/\ell_0^2$,[18,23] where k_B is the Boltzmann constant and T is the temperature.

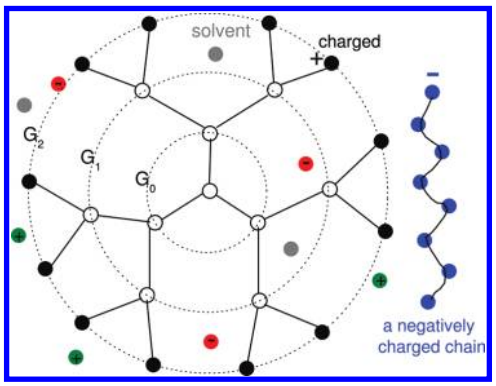

Figure 1. A sketch of our model. Monomers of the terminal generation are positively charged (black beads). Cations, anions, and solvent molecules are represented by green, red, and gray beads, respectively. A negatively charged polyelectrolyte (blue beads) was placed close to the dendrimer. The complexes between a terminally charged dendrimer of the fourth generation and a negatively charged chain with length of 16 monomers in our model were studied. The number of cations and anions is 16 and 48 in our system, respectively.

Meanwhile, the harmonic bond angle potential is included to represent the intrinsic stiffness of linear PE chains[28]

$$U_{\text{angle}}(r) = \frac{1}{2}K_\theta(\theta - \theta_0)^2 \tag{2}$$

where θ is the bond angle between three consecutive monomers and the equilibrium bond angle θ_0 is equal to 180°. A few values of the spring constants K_θ have been used to represent the different stiffness of PE.

All particles including the solvent molecules in our simulation system interact through the purely repulsive truncated-shifted LJ potential (good solvent) given by

$$U_{\text{LJ}}(r) = \begin{cases} 4\epsilon\left[\left(\frac{\sigma}{r}\right)^{12} - \left(\frac{\sigma}{r}\right)^{6} + \frac{1}{4}\right] & r \le \sqrt[6]{2}\sigma \\ 0 & r > \sqrt[6]{2}\sigma \end{cases} \tag{3}$$

where r is the separation distance between the centers of particles and ϵ and σ are the LJ energy and length scales, respectively. In our model, we assume the same LJ length for interactions between all particle pairs. Here, we set $\epsilon = 0.3k_BT$ and $\sigma = 0.8\ell_0$.[23]

All charged particles also interact through Coulomb interactions

$$U_{\text{Coul}}(r) = k_B T l_B \frac{q_i q_j}{r} \tag{4}$$

where q_i and q_j are the valences of particles i and j with a separation r. l_B is the Bjerrum length defined as the length at which the electrostatic energy of two unit charges equals to the thermal energy. It can be expressed as $l_B = e^2/(4\pi\varepsilon_0\varepsilon_r k_B T)$, where e is the elementary charge, ε_0 is the permittivity of vacuum, and ε_r is relative dielectric constant of the solvent.

We study a linear PE chain composed of 16 monomers. The seven bond angle constants, K_θ, are varied as follows: 0.0, 5.0, 10.0, 20.0, 40.0, 70.0, and 140.0 k_BT/rad^2 for exploring the effects of the rigidity of chain (from the flexible to stiff). In addition, to represent different dielectric permittivities of environments, we choose two Bjerrum lengths, i.e., $1.3l_0$ (e.g., water solution) and $10.0l_0$ (e.g., hydrophobic core of cell membranes).[23] For reference, the simulations of isolated PEs and dendrimers with their counterions in solution are also performed.

Initial configurations of dendrimers were generated via using the procedure suggested by Murat and Grest.[29] A linear PE chain was placed nearby the dendrimer. Counterions and solvent molecules were randomly inserted in the simulation box with all particles concentration $C = 1.688/_0{}^{-3}$. The simulations were performed using the open source software LAMMPS[30] with a cubic box size of $17.75/_0$ under periodic boundary conditions along three directions. For large K_θ(40, 70, 140), the box size is increased to $35.5/_0$ in order to avoid the finite size effect. The long-range electrostatic interactions were handled by the particle−particle particle−mesh (PPPM) method[31] with the sixth-order charge interpolation scheme. The particles were assumed to have the same mass m. After prepared initial configurations, each system was subjected to 1000 steps of conjugate gradient minimization of potential energy. Then the simulation was run orderly 10^6 time steps in Langevin thermostat with the time step 0.005τ and 10^6 time steps in Berendsen thermostat with the time step 0.0024τ, where $\tau = (ml_0{}^2/\epsilon)^{1/2}$ is the time unit of our model. Finally, the configurations of complexes were collected every 10^3 time steps in constant energy (NVE) ensemble with the time step 0.0012τ as previous work,[23] and the total product runs of each case are 10^7 time steps.

III. Results and Discussion

A. Radii of Gyration. It has been suggested that the charged nanoparticles can embed in membrane and may induce a hole formation depending on their sizes.[32] It is very interesting to study the size of dendrimers (soft nanoparticles) as well as PE in the complexes. We use the mean-square radius of gyration to characterize the sizes of the PE and the charged dendrimer. The mean-square radius of gyration, $\langle R_g{}^2\rangle$, is calculated by the equation

$$\langle R_g{}^2\rangle = \left\langle \frac{1}{N}\sum_{i=1}^{N} (\vec{r}_i - \vec{r}_{cm})^2 \right\rangle \quad (5)$$

where N is the number of monomers on the linear PE or on the dendrimer, $\vec{r}_i$ is the position vector of the ith monomer, and $\vec{r}_{cm}$ is the center of mass of the PE or the dendrimer in the complexes.

Figure 2 shows $\langle R_g{}^2\rangle$ of the PE and the whole dendrimer as a function of PE rigidity under two different dielectric permittivity conditions, namely the Bjerrum length is $1.3l_0$ and $10.0l_0$. We also plot the $\langle R_g{}^2\rangle$ of isolated PEs as references. With the increase in the PE stiffness, one expects that the size of PE chain in the complexes increases at both strengths of electrostatic interactions. This indicates that the compaction of PE induced by the charged dendrimer becomes troublesome due to the increase in elastic energy of PE originating from its bending as the reduced spring constant κ ($\kappa = K_\theta/(k_BT/\text{rad}^2)$, which is a dimensionless quantity) increases. This result is also manifested by comparing the $\langle R_g{}^2\rangle$ of PE with dendrimer and without dendrimer. At each κ, we can also observe that $\langle R_g{}^2\rangle$ of PE at $l_B/l_0 = 10.0$ becomes smaller with respect to that at $l_B/l_0 = 1.3$ in the complexes due to a stronger electrostatic interaction between the PE and other charged particles including terminally charged monomers of dendrimer and counterions of PE. Similarly, the size of dendrimer in the case of $l_B/l_0 = 10.0$ is smaller than that in the case of $l_B/l_0 = 1.3$ at each κ. The result is in agreement with the finding of Lyulin et al.[18,23] They demonstrated that the size of dendrimer decreases with increasing the strength of electrostatic interactions when $l_B > 1.0l_0$ in the complexes, possibly due to the effect of multipole attraction between different parts of dendrimer caused by the condensed counterions of dendrimer. This implies that the conformations of dendrimers show more collapse in the hydrophobic core of cell membranes with respect to that in the bulk of polar solvent in spite of stiffness of bioactive guests attached on the dendrimer.

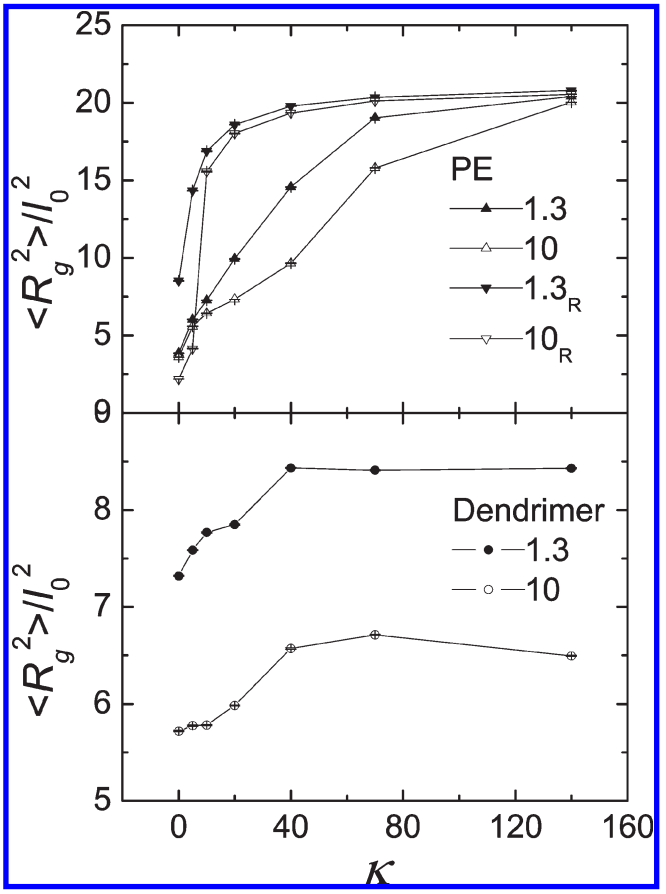

Figure 2. Mean-square radii of gyration, $\langle R_g{}^2\rangle$, of the linear PE and the charged dendrimer in the complexes as a function of PE rigidity, κ, with the chosen Bjerrum lengths $l_B/l_0 = 1.3$ and 10.0. The dimensionless quantity, κ, is equal to $K_\theta/(k_BT/\text{rad}^2)$. In addition, the $\langle R_g{}^2\rangle$s of the isolated PEs for $l_B/l_0 = 1.3$ (▼) and 10 (▽) and error bars are also presented. The $\langle R_g{}^2\rangle$ of the dendrimer without the PE is $7.93l_0{}^2$ at $l_B/l_0 = 1.3$ as well as $5.18l_0{}^2$ at $l_B/l_0 = 10$.

What is more interesting is the fact that the size of the dendrimer depending on the PE rigidity is not monotonic at both Bjerrum lengths; i.e., $\langle R_g{}^2\rangle$ of dendrimer increases with the increase of PE stiffness when κ is below 40, and then it slightly decreases with increasing κ further (Figure 2). As we know, dendrimer possesses the internal conformational degrees of freedom because of its intermediate nature between polymer and colloid. In the complexes, the conformation of PE gradually unfolds with the increase of the elastic energy among PE's segments via increasing κ; this drives the expansion of the conformation of dendrimer because of the strong electrostatic interactions between the PE chain and the terminal monomers of the dendrimer. But for stronger stiffness, PE seems like a rod which lowers the average number of PE monomers condensed onto the dendrimer due to the decrease of contact area, and then the electrostatic interactions between them are weakened. As a result, the size of dendrimer decreases as the size of PE increases. This also implies that the PE stiffness reduces its ability for directing the collapse of charged dendrimer. For isolated dendrimer, the $\langle R_g{}^2\rangle$ at $l_B/l_0 = 1.3$ is about $7.9l_0{}^2$. It is slightly larger than the finding of work[15] which is in the framework of implicit solvent model, but it is in accordance with the finding of all-atomic simulations.[33]

Comparing the sizes of PEs and dendrimers at the same value of κ, we can witness that the size of PE is larger than the size of dendrimer when κ is beyond a critical value at both Bjerrum lengths; e.g., the $\langle R_g^2 \rangle$ of PE is smaller than that of dendrimer when $\kappa \leq 20$ and is larger when $\kappa > 20$ at $l_B/l_0 = 1.3$. This reveals that a cationic dendrimer can be considered as rather effective vector for compaction of flexible bioagents, while it does not seem to be appropriate for packing relatively long stiff bioactive agents. Therefore, one needs more dendrimers[34] to protect the bioactive agents from degradation within the extracellular environment, since it is an important prerequisite for efficient drug and gene delivery.[1,2]

B. Shape Anisotropy. It has been demonstrated that the shape of nanoparticles for drug delivery is very important for the membrane permeability and the maximal intracellular uptake.[35,36] Dendrimer is a soft nanoparticle. As a host, the shape of dendrimer can be affected by other guest molecules. Thus, the asphericity, which can be used to quantitatively analyze the shape of the complexes, is another very interesting quantity. Generally, the instantaneous shape of macromolecules can be analyzed quantitatively by means of the radius of gyration tensor

$$\mathcal{R}_{\alpha\beta} = \frac{1}{N}\left[\sum_{i=1}^{N}(r_{i,\alpha} - r_{cm,\alpha})(r_{i,\beta} - r_{cm,\beta})\right] \quad (6)$$

where α and β ($= x$, y, or z) are the three Cartesian components and $r_{i,\alpha}$, $r_{cm,\alpha}$ as well as $r_{i,\beta}$, $r_{cm,\beta}$ are the coordinates of the ith monomer and of the center of mass of macromolecules, respectively. The two invariants $I_1 = I_x + I_y + I_z$, $I_2 = I_xI_y + I_yI_z + I_zI_x$ are used to define the asphericity $a = 1 - 3\langle I_2/I_1^2 \rangle$, where I_x, I_y, I_z are the three eigenvalues, corresponding to the three semiaxes of equivalent ellipsoid, of the $\mathcal{R}_{\alpha\beta}$; the brackets, $\langle\,\rangle$, stand for the ensemble average. The value of a is between 0 and 1. Specifically, $a = 0$, 1/4, and 1 represent spherical, oblate, and extremely elongated ellipsoids, respectively.

The stiffness effect of PE on its asphericity is shown in Figure 3. In the absence of charged dendrimer, the a increases monotonically with the increasing of κ at both l_B due to the increase in bending energy. However, it is shown that the asphericity of PE exists a slight decrease as κ increases from 0 to 5 at both Bjerrum lengths in the complex. As κ increases further, the asphericity of PE increases from 0.25 to 1.0. This indicates that the shape of PE in the complexes exists a slight fluctuation around oblate object at small value of κ, where the elastic energy of PE is not comparable with electrostatic attractive interactions. When the inherent elastic energy of PE is comparable and beyond the electrostatic interaction energy between PE and dendrimer ($\kappa \geq 70$), the PE displays a prolate or "rodlike" shape.

Meanwhile, the effect of the conformational change of PE on the dendrimer in the complex is also shown. We can observe that the asphericity of dendrimer in the complex increases from 0.05 to 0.08 with increasing the PE rigidity when κ is below 40 at the Bjerrum length of $1.3l_0$. With further increasing κ, the value of a of the dendrimer only shows a slight increase. All asphericity values are less than 0.1, implying that the dendrimer does not take on conformations deviating by a large amount from a spherical shape at $l_B/l_0 = 1.3$. In the case of Bjerrum length equal to $10.0l_0$, the value of a increases from 0.05 to 0.16 with the increase of κ (below 70). What is more interesting is that the asphericity of dendrimer decreases as κ increases further (above 70). The above results indicate that the PE rigidity has a stronger impact on the shape of dendrimer at $l_B/l_0 = 10.0$ than at $l_B/l_0 = 1.3$. Furthermore, we witness that the asphericity of dendrimer at $l_B/l_0 = 10.0$ is larger with respect to that at $l_B/l_0 = 1.3$, especially when $\kappa = 70$. This suggests that the conformations of dendrimer gradually depart spherical shape as the complexes approach the cell membrane because of the increase in the strength of electrostatic interaction. In our model, the shape change of dendrimer is induced by electrostatic interactions between the charged dendrimer and PE with the various conformations, unlike that induced by the increase of generation number, which is possibly owing to the steric and entropic effects.[37] In the absence of PE, the a of the charged dendrimer is near 0.045 at both Bjerrum lengths. This is in good agreement with the finding of all-atomic simulations of Maiti et al.[38]

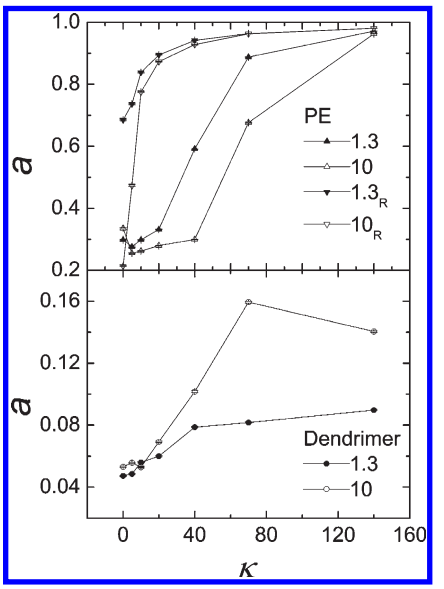

Figure 3. Average relative shape anisotropy of the PE chain and the dendrimer, a, as a function of rigidity of PE, κ, for the specified Bjerrum lengths $l_B/l_0 = 1.3$ and 10.0. The a of the isolated dendrimer is 0.047 at $l_B/l_0 = 1.3$ as well as 0.044 at $l_B/l_0 = 10$.

Furthermore, we also calculate the average aspect ratios defined as $a_{xy} = I_x/I_y$ and $a_{xz} = I_x/I_z$ ($I_x \geq I_y \geq I_z$) to analyze the shape change of PE and dendrimer in the complexes or as a isolated one in detail. We plot the average aspect ratios, a_{xy} and a_{xz}, of PE and dendrimer as a function of the PE rigidity in Figures 4 and 5, respectively. It can be found that a_{xy} and a_{xz} of the isolated PE increase with the increase of κ at both Bjerrum lengths, and it is the same with that of PE in the complex. However, the a_{xy} and a_{xz} of PE in the complex are smaller than that of an isolated PE at a given κ, which indicates that the charged dendrimer has an ability to change the conformation of PE in the complex to a certain extent due to the electrostatic attraction. The amount of a_{xz} is about 10 times larger than a_{xy} at larger κ (>10) at both Bjerrum lengths. Accordingly, these average aspect ratios support the shape of PE transforming from oblate to prolate with increasing its stiffness and also are a manifestation of unfolding of PE. As for dendrimer (see Figure 5), we find that within κ studied the values of a_{xy} are between 1.4 and 1.7, and the values of a_{xz} are between 2.1 and 3.0 at the Bjerrum length of $1.3l_0$. For the Bjerrum length of $10.0l_0$, the values of a_{xy} are between 1.4 and 2.5, and the values of a_{xz} are between 2.1 and 3.9. This means that the shape of dendrimer shows a slight change with the increase of κ at $l_B/l_0 = 1.3$ with respect to that at $l_B/l_0 = 10.0$, consistent with the result that the PE rigidity has a stronger impact on the shape of dendrimer at $l_B/l_0 = 10.0$ than at $l_B/l_0 = 1.3$.

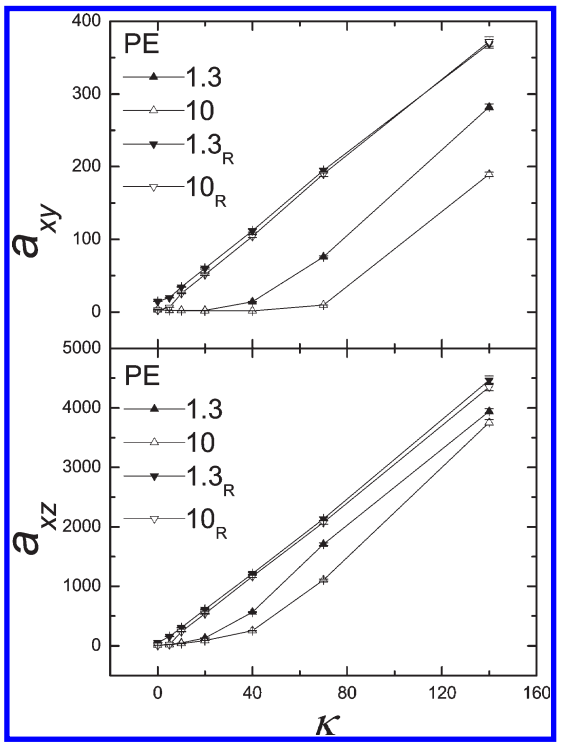

Figure 4. Average aspect ratios a_{xy} and a_{xz} of PEs as a function of rigidities of PEs for the specified Bjerrum length $l_B/l_0 = 1.3$ and 10.0.

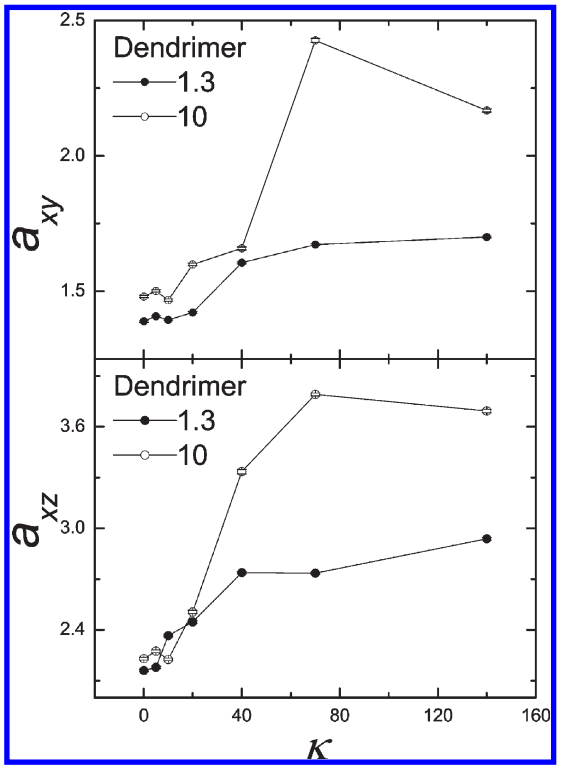

Figure 5. Average aspect ratios a_{xy} and a_{xz} of dendrimers as a function of rigidities of PEs for the specified Bjerrum length $l_B/l_0 = 1.3$ and 10.0. The a_{xy} for the isolated dendrimer is 1.42 at $l_B/l_0 = 1.3$ as well as 1.35 at $l_B/l_0 = 10$. Meanwhile, the a_{xz}'s of the isolated dendrimers at both Bjerrum lengths are 2.14 and 2.12, respectively.

Snapshots of the typical conformations of dendrimer−chain complexes with the specified PE stiffness at $l_B/l_0 = 1.3$ are displayed in Figure 6. It is very interesting to see that the chain of PE collapses into the actual domain of charged

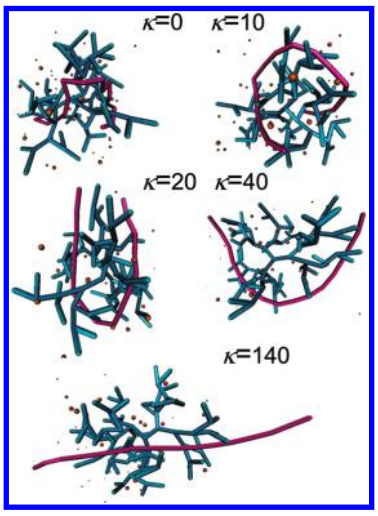

Figure 6. Snapshots, generated with the Visual Molecular Dynamics (VMD) package,[39] of the dendrimer−chain complexes with the specified rigidities of PEs at $\kappa = 0$, 10, 20, 40, and 140 for the case $l_B/l_0 = 1.3$.

dendrimer at $\kappa = 0$, consistent with the finding of Lyulin et al.[23] for flexible PE. As the PE stiffness increases, the conformation of PE changes from "coil"-like ($\kappa = 10$) to "U"-like ($\kappa = 20$) or "V"-like ($\kappa = 40$) and further to "rod"-like ($\kappa = 140$). This is a clear manifestation of unfolding of the conformation of PE. The above conformations of PE were also found in the previous theoretical modeling[40] and computer simulations,[41−44] which focused on the complexes of hard spheres and PEs. This can be explained as a consequence of several competing effects: the electrostatic attractive interactions between the PE and the monomers of dendrimer force the chain to collapse and penetrate into the dendrimer, while the electrostatic repulsion between the chain monomers and the intrinsic chain rigidity forces the PE to undergo a structural transition and adopt an extended conformation. In our model, the bond length $l_0 \simeq 6.7$ Å,[23] and the intrinsic persistence length which is a basic mechanical property quantifying the stiffness of a PE, can be estimated by $L_p \simeq K_\theta l_0/2k_BT$.[28] Thus, the persistence length for $\kappa = 10.0$ and 140.0 is equal to 33.5 Å (experimental values of ssDNA ranging from 7.5 to 30) and 469.0 Å (experimental values of dsDNA ≃ 500), respectively. The coil-like and rod-like conformations are in harmony with the findings of atomistic simulation of Mariti et al.[24,34] for the complexes formed by dendrimer and ssDNA or dsDNA.

C. Effective Charge. The overcharging phenomenon, which is very interesting in colloid and surface science, has attracted considerable attention because it is with potential relevance to the development of biological applications.[45,46] To clarify the impact of the PE rigidity on the effective charge of dendrimer, we calculate the number of adsorbed negative particles for all the systems studied. If a particle has a terminal monomer of the dendrimer in its first coordination shell, we consider it to be condensed on the dendrimer. To evaluate the size of the shell, we first calculate the radial distribution functions for particles between the dendrimer monomers and the PE monomers as well as the counterions of dendrimer. The radius of the first coordination shell is then extracted from the position of first minima in the radial distribution functions. This method was used by the previous studies.[18,23,47] We find that the radii are the same for the above particles in all the systems and are nearly equal to $1.3l_0$, consistent with the previous study.[23]

Generally, we find that the effective charge does not change significantly at small κ, where the bending energy is

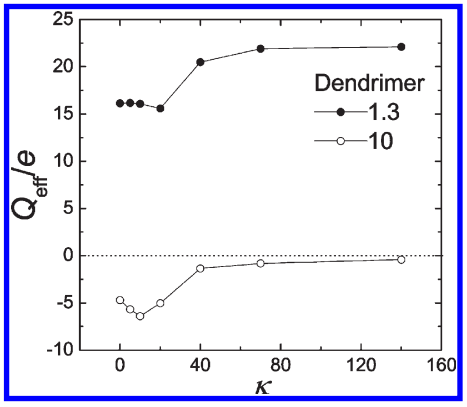

Figure 7. Effective charge of a cationic dendrimer Q_{eff} as a function of PE rigidity, κ, for the specified Bjerrum lengths $l_B/l_0 = 1.3$ and 10.0.

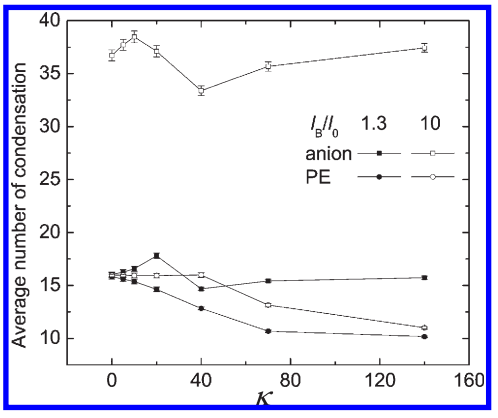

Figure 8. Average number of condensed counterions (anions) of the dendrimer and the monomers of PE on the dendrimer as a function of PE rigidity, κ, for the specified Bjerrum lengths $l_B/l_0 = 1.3$ and 10.0. Note that the number of cationic monomers of one dendrimer is 48.

minor relative to electrostatic interaction (see Figure 7). At large κ where the bending energy of PE is beyond the electrostatic interactions between the monomers of PE and the terminal monomers of dendrimer, the effective charge does not change significantly either. It is very interesting that the Q_{eff} exists a jump between $\kappa = 20$ and 70 at $l_B/l_0 = 1.3$, while the jump of Q_{eff} is between $\kappa = 10$ and 40 at $l_B/l_0 = 10.0$. The above behavior of Q_{eff} origins from the change of the condensed counterions of dendrimer and anionic monomers of PE on the dendrimer (see Figure 8). When $l_B/l_0 = 1.3$, the average number of condensed monomers of PE decreases with the increase of κ because of its unfolding. At small κ, the average of condensed counterions of dendrimer slightly increases with the increase of κ because of the following two reasons: the decrease in the number of PE monomers and the increase in the size of dendrimer, which provides a large interface or volume for the counterions of dendrimer being trapped. The effects of entropy due to the increase in the volume of system lead to the decrease in the average number of condensed counterions between $\kappa = 20$ and 40. It should be noted that the effect of entropy is not the dominating reason, instead of the unfolding of PE, for the appearance of jump of Q_{eff}. When $\kappa > 40$, the average number of condensed anions increases with the increasing of κ, mainly due to the unfolding of PE induced by the increase of its inherent persistent length. This means that the decrease of the condensed monomers of PE is compensated by the counterions of dendrimer to neutralize the charge of dendrimer. The occurrence of jump of Q_{eff} is mainly because that, with the increase in κ from 20 to 70, the number of condensed monomers of PE decreases about 5, which is 2 times more than that of anions. As for $l_B = 10.0l_0$, the condensed number of anions increases and that of monomers of PE nearly keeps unchanged at small κ (≤ 10), which can explain the slight deceasing of effective charge of dendrimer at the small κ (see Figure 7). As the PE chain changes from flexible to rigid, there may exist a zone of Bjerrum lengths, at which the effective charge is negative at small κ but positive at large κ.

As expected, the number of condensed anion at the large Bjerrum length is more than that at small one, which is a main reason for the difference of Q_{eff} at different Bjerrum lengths, because of stronger electrostatic interactions between the charged monomers of dendrimer and its counterions (see Figure 8). Consequently, the effective charge of dendrimer is positive at $l_B = 1.3$ while it is negative at $l_B = 10.0$. In other words, we witness a noticeable overcharging for the dendrimer in the complexes, regardless of the value of κ at the large Bjerrum length. This result contrasts with the findings of a recent simulation study by Majtyka and Klos,[48] who studied single charged dendrimers under the presence of mono- and divalent salt but did not observe overcharging of dendrimers. However, the present result agrees with the finding of Lyulin et al.,[23] who studied the complex of dendrimer and short flexible PE chain, and the finding of our previous work[49] which paid attention to a charged dendrimer in multivalent salt solution. It should be stressed that this charge inversion of dendrimer in the complexes reduces its potential ability to binding to the healthy cell membrane which carries a net negative charge of about 0.02 C/m^2,[50] because of the electrostatic repulsion between the complexes with negatively effective charge and membrane. There may exhibit a overcharging phenomenon,[23] as the dendrimer−chain complexes approach the membrane from water phase to membrane interior. Thus, this approaching process will become more and more troublesome due to the unfavorable electrostatic repulsion.

D. Radial Number Distribution. The location of the PE chain relative to the dendrimer is very relevant to drug and gene delivery. We use the component-wise distributions for the number of particles in complex as a function of the radial distance r from the center of mass of the dendrimers to analyze this property (see Figure 9). First, the terminal monomers are found to be broadly distributed at all κ studied here, implying considerable backfolding. This result is in full agreement with the findings of previous studies[18,23,24] due to the entropy effect of the terminal monomers. Second, we find that the peak of the distribution of PE particles shifts away from the center of mass of the dendrimer as κ increases. This strongly suggests that the stiffer the PE, the closer to the dendrimer surface it is. Further, we can also see that the distribution is not zero in the exterior of the dendrimer when κ is beyond a critical value. This is most likely because the electrostatic interaction energy between PE and dendrimer cannot effectively induce the bending of the stiff PE due to the large bending energy. This finding is another manifestation of our conclusion that a dendrimer cannot effectively compact a stiff bioagents for protecting them from the surrounding medium. Furthermore, the distributions of counterions of dendrimer at the large values of κ (= 40, 70) also give insight into that there are more counterions of dendrimer trapping in the dendrimer with the increasing of κ, which has been demonstrated by the average number of condensed anions. Moreover, cations (data not shown) are mainly distributed around the charged dendrimer at all κ's studied because of the electrostatic repulsions between cations and terminal monomers of dendrimer.

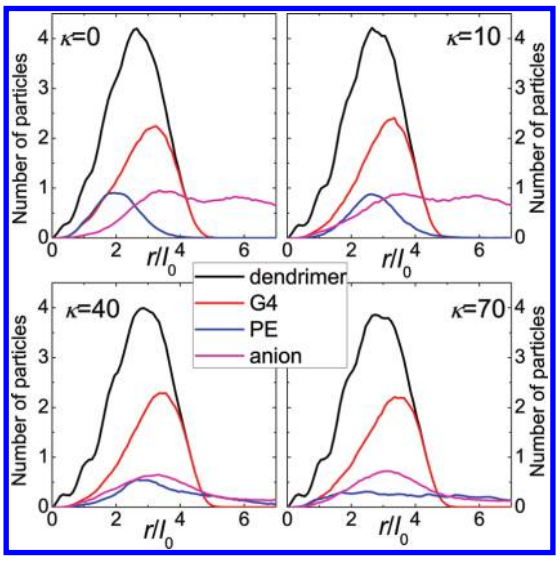

Figure 9. Distributions for the number of particles as a function of the radial distance r from the center of mass of the dendrimer for the specified PE rigidities in the case of $l_B = 1.3$. Shown are results for the whole dendrimer, terminal monomers (G4), chain (PE), and counterions of the dendrimer (anions). For the sake of clarification, counterions of PE (cations) are not shown.

The distribution of PE relative to the dendrimer at small κ also demonstrates the penetration of PE into the dendrimer. This result is in excellent agreement with that of Maiti et al.,[24] who found the complete penetration of the almost whole ssDNA into G4 dendrimer with atomistic molecular dynamics simulations. Such a penetration effect is important for protecting guest molecules, but a strong penetration of a guest into a dendrimer may complicate the guest release, which would make the use of the dendrimers as nanocarriers difficult, although there exist other methods for controlling the release, such as changing the pH of systems.[24] In addition, the stiffer the PE, the closer to the surface of dendrimer it is. A large stiffness induces some of the monomers of PE to be exposed to solvent. Hence, we expect that there may exist the most optimal stiffness of relatively short bioactive guests for delivery and release, whereas we cannot give the optimum parameter on the basis of our simple model. The guest at the most optimal stiffness cannot be degraded in the process of delivery due to the penetration into the host (dendrimer) but can be easily released due to modest penetration as it reaches the target.

The conformational change of dendrimer with varying the PE stiffness also suggests that, to a certain extent, it is not reasonable to treat the charged dendrimer as an impenetrable hard sphere[51−55] with fixed size. This conclusion is consistent with that of Qamhieh et al.,[56] who investigated the interaction between positively charged dendrimers of G4 and very long DNA via a theoretical model. On the basis of the experimental data,[57] they treated the dendrimer as a soft sphere and found that the optimal number of dendrimers per DNA decreases for smaller dendrimer radii, meaning that the more compressed the dendrimer becomes upon DNA interaction, the less dendrimers will bind the DNA molecule due to the increased cost in the elastic (bending) free energy. Their results pronouncedly suggested that the dendrimer should not be modeled as a hard sphere with a fixed radius. It should be pointed out that the length of PE in the present model is much shorter than that of Qamhieh et al.;[56] understanding the effects of PE length is a very interesting issue for further research.

Generally speaking, dendrimer (nanoparticle)−chain complexes are interesting in that they combine the subtle interplay between electrostatic interactions and elastic energy as well as entropic effects due to conformational changes of the PE chain, leading to a wide range of structural properties. Here, we only focus on the electrostatic interactions among charged monomers and the stiffness effect of PE. The inner-dendrimer hydrophobic components may play different roles in the morphology changes and binding structures of the dendrimer in the complexes. Besides, studies of other factors such as solvent quality, size of nanoparticles (generation of dendrimers), ion valency, and concentration are also needed to clarify their roles in the size, shape, and effective charge of dendrimer in the complexes. Furthermore, a further improvement of our dendrimer model through incorporating the angle and torsional potentials is very important to diminish the discrepancies between the coarse-grained model and the atomic-scale simulations or experimental data. Moveover, the simulation box in our model was enlarged at large κ. Although some free ions will move away the charged dendrimer due to the entropy effect, the increase of box does not have a significant change of the ambiance of dendrimer because the effective screening length is associated with the local region rather than the bulk region.[15] Additionally, there are only two main competing interactions in our system: electrostatic energy and bending energy. As the κ of PE increases, there exists the transition of dominant interactions from the electrostatic energy to the bending energy at a given Bjerrum length. Thus, we believe that the electrostatic interaction induced by box change only is slightly strengthened around the dendrimer, and it will not change our conclusion except a slight change of κ at which the transformation of PE conformation and the jump of effective charge appear.

IV. Conclusions

We investigate the effects of chain stiffness on the complexes between a cationic dendrimer of the fourth generation and an anionic PE chain by means of molecular dynamics simulations with explicit free ions in a framework of an extensive coarse-grained model for the dendrimer and the PE where solvent molecules are also incorporated. To the best of our knowledge, this is the first coarse-grained computational investigation of complexes between dendrimer and linear PE of various rigidities. We pay attention to the influence of the PE stiffness on the size, shape, effective charge of dendrimer, and the distribution of PE monomers relative to the dendrimer because of their relationship to the toxicity and efficiency of nanoscale "drug" carriers.

We find that the size of PE chain increases and the shape changes from oblate to prolate concomitant with the interesting conformational transformations from "coil"-like to "U"-like or "V"-like and then to "rod"-like due to the increase in bending energy with increasing the PE stiffness in the complexes. We also find that the size of dendrimer increases with the unfolding of the structure of PE at small κ. At large κ, the size of dendrimer is not sensitive to the PE stiffness at the small Bjerrum length while that shows a slight decrease with the increasing of the value of κ at a larger Bjerrum length. Further, the spherical shape of dendrimer shows a slight change with the changing of PE's conformation at the small Bjerrum length but displays a pronounced change at the larger Bjerrum length. This can be explained as a result of several competing factors: the electrostatic repulsions between the PE monomers and the intrinsic chain rigidity induce the PE to undergo a structural transition and adopt extended conformations; the electrostatic attractive interactions between the PE and the dendrimer force the PE to bend and penetrate into the dendrimer; and the structure of PE also impacts the conformation of dendrimer in the complexes. Furthermore, we witness that

the effective charge of dendrimer exists a jump at both Bjerrum lengths studied here, but the overcharging phenomenon only occurs at the large Bjerrum length due to stronger electrostatic interactions between dendrimer and anionic particles including counterions of dendrimer and monomers of PE. Moreover, the radial number distributions demonstrate that the stiffer the PE, the closer to the dendrimer surface it is. Some of the PE monomers will be exposed to the outer environment when the stiffness of the PE reaches a certain degree.

Our results indicate that the compaction and penetration of PE induced by charged dendrimer become troublesome when the PE becomes stiff with the increasing of elastic energy and that the stiffness of PE reduces its ability for propelling the collapse of charged dendrimer. Therefore, a cationic dendrimer can be considered as an effective vector for compaction of flexible anionic bioagents, but it should need more dendrimers to protect the stiff bioactive molecules, such as DNA, from degradation for delivery. We speculate that there may exist the most optimum stiffness of bioactive guests for delivery and release. In addition, it should be unreasonable to treat the charged dendrimer as an impenetrable hard sphere with a fixed size.

Finally, understanding the complexes formed by the charged dendrimers (or other nanoparticles) and bioactive molecules through the cell membrane is a subject of interest in improving drug and gene delivery vehicles. It has been suggested that there is a finite region of parameter space in which a complex may successfully land on a cell membrane and stay intactly long enough for cellular entry to occur.[58] Thus, understanding of the transit process of dendrimer−PE complexes through a lipid bilayer[59] is an important issue addressed in our further work.[60]

Acknowledgment. This work was supported by the National Basic Research Program of China, No. 2007CB925101, and the National Natural Science Foundation of China, Nos. 10974080, 20674037, and 10629401. We are grateful to the High Performance Computing Center of Nanjing University for the award of CPU hours to accomplish this work. W.T. is grateful to Dr. Xiao-yu Chen for her careful reading of this manuscript.

References and Notes

(1) D'Emanuele, A.; Attwood, D. *Adv. Drug Delivery Rev.* **2005**, *57*, 2147.
(2) Dykes, G. M. *J. Chem. Technol. Biotechnol.* **2001**, *76*, 903.
(3) Svenson, S.; Tomalia, D. A. *Adv. Drug Delivery Rev.* **2005**, *57*, 2106.
(4) Parrott, M. C.; Benhabbour, S. R.; Saab, C.; Lemon, J. A.; Parker, S.; Valliant, J. F.; Adronov, A. *J. Am. Chem. Soc.* **2009**, *131*, 2906.
(5) Ballauf, M.; Likos, C. N. *Angew. Chem., Int. Ed.* **2004**, *43*, 2998.
(6) Helms, B.; Meijer, E. W. *Science* **2006**, *313*, 929.
(7) Tang, M. X.; Redemann, C. T.; Szoka, F. C. *Bioconjugate Chem.* **1996**, *7*, 703.
(8) Shi, X.; Wang, S. H.; Swanson, S. D.; Ge, S.; Cao, Z.; Van Antwerp, M. E.; Landmark, K. J.; Baker, J. R. *Adv. Mater.* **2008**, *20*, 1671.
(9) Leroueil, P. R.; Hong, S.; Mecke, A.; Baker, J. R.; Orr, B. G.; Holl, M. M. B. *Acc. Chem. Res.* **2007**, *40*, 335.
(10) Nel, A. E.; Madler, L.; Velego, D.; Xia, T.; Hoek, E. M. V.; Somasundaran, P.; Klaessig, F.; Castranova, V.; Thompson, M. *Nat. Mater.* **2009**, *8*, 543.
(11) Nel, A. E.; Xia, T.; Madler, L.; Li, N. *Science* **2006**, *311*, 626.
(12) Mitragotri, S.; Lahann, J. *Nat. Mater.* **2009**, *8*, 15.
(13) Lee, H.; Larson, R. G. *Molecules* **2009**, *14*, 423.
(14) Lee, H.; Larson, R. G. *J. Phys. Chem. B* **2008**, *112*, 12279.
(15) (a) Lee, I.; Athey, B. D.; Wetzel, A. W.; Meixner, W.; Baker, J. R. *Macromolecules* **2002**, *35*, 4510. (b) Lyulin, S. V.; Evers, L. J.; Van der Schoot, P.; Darinskii, A. A.; Lyulin, A. V.; Michels, M. A. J. *Macromolecules* **2004**, *37*, 3049. (c) Karatasos, K.; Krystallis, M. *J. Chem. Phys.* **2009**, *130*, 114903.
(16) (a) Lee, H.; Baker, J. R.; Larson, R. G. *J. Phys. Chem. B* **2006**, *110*, 4014. (b) Maiti, P. K.; Messina, R. *Macromolecules* **2008**, *41*, 5002.
(17) (a) Giupponi, G.; Buzza, D. M. A.; Adolf, D. B. *Macromolecules* **2007**, *40*, 5959. (b) Blaak, R.; Lehmann, S.; Likos, C. N. *Macromolecules* **2008**, *41*, 4452.
(18) Gurtovenko, A. A.; Lyulin, S. V.; Karttunen, M.; Vattulainen, I. *J. Chem. Phys.* **2006**, *124*, 094904.
(19) Welch, P.; Muthukumar, M. *Macromolecules* **2000**, *33*, 6159.
(20) Lyulin, S. V.; Karatasos, K.; Darinskii, A.; Larin, S.; Lyulin, A. V. *Soft Matter* **2008**, *4*, 453–457.
(21) Lyulin, S. V.; Darinskii, A. A.; Lyulin, A. V. *Macromolecules* **2005**, *38*, 3990.
(22) Lyulin, S. V.; Darinskii, A. A.; Lyulin, A. V. *Phys. Rev. E* **2008**, *78*, 041801.
(23) Lyulin, S. V.; Vattulainen, I.; Gurtovenko, A. A. *Macromolecules* **2008**, *41*, 4961.
(24) Maiti, P. K.; Bagchi, B. *Nano Lett.* **2006**, *11*, 2478.
(25) Pincus, P. *Macromolecules* **1991**, *24*, 2912.
(26) Netz, R. R.; Andelman, D. *Phys. Rep.* **2003**, *380*, 1.
(27) Hu, J.; Cheng, Y.; Ma, Y.; Wu, Q.; Xu, T. *J. Phys. Chem. B* **2009**, *113*, 64.
(28) Stevens, M. J. *Biophys. J.* **2001**, *80*, 130.
(29) Murat, M.; Grest, G. S. *Macromolecules* **1996**, *29*, 1278.
(30) Plimpton, S. J. *J. Chem. Phys.* **1995**, *117*, 1.
(31) (a) Deserno, M.; Holm, C. *J. Chem. Phys.* **1998**, *109*, 7678. (b) Deserno, M.; Holm, C. *J. Chem. Phys.* **1998**, *109*, 7694.
(32) Ginzburg, V. V.; Balijepalli, B. *Nano Lett.* **2007**, *7*, 3716.
(33) Maiti, P. K.; Cagin, T.; Lin, S. T.; Goddard, W. A.III *Macromolecules* **2005**, *38*, 979.
(34) http://www.physics.iisc.ernet.in/∼maiti/dna_den.html.
(35) Chithrani, B. D.; Ghazani, A. A.; Chan, W. C. W. *Nano Lett.* **2006**, *6*, 662.
(36) Leroueil, P. R.; Berry, S. A.; Duthie, K.; Han, G.; Rotello, V. M.; McNerny, D. Q.; Baker, J. R.; Orr, B. G.; Holl, M. M. B. *Nano Lett.* **2008**, *8*, 420.
(37) Klos, J. S.; Sommer, J. U. *Macromolecules* **2009**, *42*, 4878.
(38) Maiti, P. K.; Cagin, T.; Wang, G. F.; Goddard, W. A.III *Macromolecules* **2004**, *37*, 6236.
(39) Humphrey, W.; Dalke, A.; Schulten, K. *J. Mol. Graphics* **1996**, *14*, 33.
(40) Netz, R. R.; Joanny, J. F. *Macromolecules* **1999**, *32*, 9026.
(41) Akinchina, A.; Linse, P. *J. Phys. Chem. B* **2003**, *107*, 8011.
(42) Akinchina, A.; Linse, P. *Macromolecules* **2002**, *35*, 5183.
(43) Wallin, T.; Linse, P. *Langmuir* **1996**, *12*, 305.
(44) Ulrich, S.; Lagueeir, A.; Stoll, S. *Macromolecules* **2005**, *38*, 8939.
(45) Grosberg, A. Y.; Nguyen, T. T.; Shklovskii, B. I. *Rev. Mod. Phys.* **2002**, *74*, 329.
(46) Messina, R. *J. Phys.: Condens. Matter* **2009**, *21*, 113102.
(47) Böckmann, R. A.; Hac, A.; Heimburg, T.; Grubmüller, H. *Biophys. J.* **2003**, *85*, 1647.
(48) Majtyka, M.; Klos, J. *Phys. Chem. Chem. Phys.* **2007**, *9*, 2284.
(49) Tian, W. D.; Ma, Y. Q. *J. Phys. Chem. B* **2009**, *113*, 13161.
(50) Bauer, J. *Cell Electrophoresis*; CRC: Boca Raton, FL, 1994.
(51) Ulrich, S.; Seijo, M.; Laguecir, A.; Stoll, S. *J. Phys. Chem. B* **2006**, *110*, 20954.
(52) Nguyen, T. T.; Shklovskii, B. I. *J. Chem. Phys.* **2001**, *115*, 7298.
(53) Schiessel, H. *Macromolecules* **2003**, *36*, 3424.
(54) Jonsson, M.; Linse, P. *J. Chem. Phys.* **2001**, *115*, 3406.
(55) Kunze, K. K.; Netz, R. R. *Phys. Rev. Lett.* **2000**, *85*, 4389.
(56) Qamhieh, K.; Nylander, T.; Ainalem, M. L. *Biomacromolecules* **2009**, *10*, 1720.
(57) Örberg, M. L.; Schillen, K.; Nylander, T. *Biomacromolecules* **2007**, *8*, 1557.
(58) Voulgarakis, N. K.; Rasmussen, K. Ø.; Welch, P. M. *J. Chem. Phys.* **2009**, *130*, 155101.
(59) (a) Li, Y.; Chen, X.; Gu, N. *J. Phys. Chem. B* **2008**, *112*, 16647. (b) Lee, H.; Larson, R. G. *J. Phys. Chem. B* **2006**, *110*, 18204.
(60) Tian, W. D.; Ma, Y. Q. Manuscript in preparation.